

An optimized protocol of high precision measurement of Hg isotopic compositions in samples with low concentrations of Hg using MC-ICP-MS

Hongyan Geng,^{ab} Runsheng Yin,^{cd} and Xiangdong Li^{ad*}

^aUniversity Research Facility in Chemical and Environmental Analysis (UCEA), The Hong Kong Polytechnic University, Hong Hum, Kowloon, Hong Kong

^bShandong Provincial Key Laboratory of Depositional Mineralization and Sedimentary Minerals, College of Geological Sciences and Engineering, Shandong University of Science and Technology, Qingdao 266590, China

^cState Key Laboratory of Ore Deposit Geochemistry, Institute of Geochemistry, Chinese Academy of Sciences, Guiyang 550002, China

^dDepartment of Civil and Environmental Engineering, The Hong Kong Polytechnic University, Hung Hom, Kowloon, Hong Kong

***Corresponding author: Xiangdong Li** (E-mail: cexdli@polyu.edu.hk; Tel: +852 2766 6041. Fax: +852 2334 6389)

Abstract

Multi-collector inductively coupled plasma mass spectrometry (MC-ICP-MS) enables the precise determination of mercury (Hg) isotopic compositions in different types of samples. However, isotopic measurements in samples with low Hg concentrations and small sample mass remain a challenge. In this study, we developed an optimized protocol for high precision Hg isotopic determination using the modified cone arrangement (X skimmer cone + jet cone) with Neptune Plus MC-ICP-MS. Through modification of the HGX-200 continuous-flow cold-vapor generation system, and careful optimization of the instrument gas flows, we obtained steady and high signal sensitivity for Hg (^{202}Hg : 1.78 V per ng mL⁻¹). Our method allowed the precise determination of low Hg solutions (0.10 ng mL⁻¹), which is the lowest according to the literature. Only 0.70 ng Hg in samples was required according to our new analytical method, which enables the direct measurement of low Hg in samples (down to 5 ng g⁻¹), after direct acid digestion treatment. Using our method, the Hg isotopic compositions of four igneous rock standard reference materials (BCR-2, BHVO-2, GSP-2, GSR-2)

were reported for the first time. The standard reference materials showed large variations of $\delta^{202}\text{Hg}$ (-1.24 ~ -2.47‰), indicating that mass dependent fractionation (MDF) of Hg isotopes occurred during magmatic processes.

1. Introduction

With the development of multi-collector inductively coupled plasma mass spectrometry (MC-ICP-MS), stable isotopes of Hg have been successfully used as tracers to understand the geochemical cycling of Hg in the environment.¹⁻³ Mercury has seven natural stable isotopes (^{196}Hg , ^{198}Hg , ^{199}Hg , ^{200}Hg , ^{201}Hg , ^{202}Hg and ^{204}Hg), which undergo both mass dependent fractionation (MDF, mostly reported as $\delta^{202}\text{Hg}$) and mass independent fractionation (MIF, mainly reported as $\Delta^{199}\text{Hg}$, $\Delta^{200}\text{Hg}$, $\Delta^{201}\text{Hg}$) during various physical, chemical, and biological processes^{1,2}. Natural samples from Earth's reservoirs have shown large variations of >10‰ in both $\delta^{202}\text{Hg}$ and $\Delta^{199}\text{Hg}$ values, which are attributed to the isotope fractionation processes.² Combining the MDF and MIF signatures of Hg, Hg isotopes can provide multi-dimensional information to identify the sources and biogeochemical pathways of Hg in various sample medium.

For Hg isotopic composition analysis, the commercial HGX-200 continuous-flow cold-vapor generation system (CETAC Technologies, USA) has been conventionally used for sample introduction to MC-ICP-MS.⁴⁻⁶ This introduction approach consists of continuously reducing of Hg in solutions by SnCl_2 and generating $\text{Hg}(0)$ vapor, which gives low matrix effect, and steady and continuous Hg signals. Such technique requires substantial amounts of Hg, but tends to greatly improve external precisions of the measurements. For samples with high Hg concentrations (i.e., $\geq 25 \text{ ng g}^{-1}$), the samples

1 can be acid digested with perfect Hg recoveries ($>90\%$), and diluted to proper Hg
2 concentrations ($0.5\text{--}5\text{ ng mL}^{-1}$) and acid concentrations ($<20\%$, v/v), and directly
3 measured using MC-ICP-MS. The results showed small uncertainties of 0.10% (2SD)
4 and 0.05% (2SD) for $\delta^{202}\text{Hg}$ and $\Delta^{199}\text{Hg}$, respectively.⁵⁻⁸ At least 5-10 mL of solution
5 is normally required for Hg isotope analysis.⁵⁻⁸

6

7 For samples with low concentrations of Hg ($< 25\text{ ng g}^{-1}$), such as igneous and
8 metamorphic rocks, however, the isotopic composition determination is challenging
9 using the conventional method. Even with 100% recovery, the dilution of acid
10 concentrations to $< 20\%$ would cause low Hg concentrations (i.e., $< 0.5\text{ ng mL}^{-1}$) that
11 are difficult for Hg isotope analysis. To solve the problem, gold trapping,⁹ activated
12 carbon trapping,¹⁰ $\text{KMnO}_4\text{+H}_2\text{SO}_4$ trapping¹¹⁻¹⁶ and chromatographic pre-
13 concentration¹⁷ have been developed to pre-concentrate Hg to proper levels ($\geq 0.5\text{ ng}$
14 mL^{-1} Hg). Although these pre-concentration techniques enabled the isotopic analysis of
15 low Hg samples, it is noteworthy that pre-concentration suffers from tedious procedures,
16 which are not only time consuming and chemical use, but also pose risks for Hg isotope
17 fractionation due to Hg loss (or contamination) in the processes. More importantly, for
18 precious samples with limited masses, such as meteorite and aerosol samples, the
19 measurement of Hg isotopic composition is not possible by acid digestion and pre-
20 concentration methods due to the limited mass of Hg in samples.

21

22 An alternative way of measuring samples with low concentrations of Hg and limited
23 sample sizes is to directly improve the Hg sensitivity in instrument. The uncertainty of
24 Hg isotope ratio decreases when the Hg signal intensity is increased, therefore the
25 improvement of Hg sensitivity will enable the precise measurement of low Hg solutions.

1 The new generation Neptune Plus MC-ICP-MS (Thermo Electron Corp, Bremen,
2 Germany), which has combined modified skimmer and sample cone geometries with
3 enhanced interface pumping configuration, has largely enhanced the ion sampling
4 efficiency and overall signal sensitivity. It is worthy to note that the signal sensitivity
5 of Hg is also dependent on the types of introduction systems and the gas flow rates. In
6 a recent study, the use of modified cones combined with an adapted cold-vapor
7 generator resulted in higher Hg sensitivity than the traditional methods, which enabled
8 the precise measurement of low Hg in solutions (0.3 ng mL^{-1}).¹⁸

9
10 In the present study, we modified the continuous-flow cold-vapor generation system
11 based on the HGX-200 system. Through careful optimization of the instrument gas
12 flows, we achieved much higher signal sensitivity of $1.78 \text{ V per ng mL}^{-1} \text{ Hg}$ for ^{202}Hg .
13 With this signal sensitivity, high precision measurement of much lower Hg solutions
14 (0.10 ng mL^{-1}) was achieved. Our method enabled the direct measurement of low Hg
15 samples (low to 5 ng g^{-1}), after the direct acid digestion treatment. Using our developed
16 method, the Hg isotope compositions of four igneous rock reference materials were
17 measured and reported for the first time. In addition, it has always been a conundrum
18 about how to optimize the Hg isotope signals because it has rarely been clearly
19 described in pervious publications. Based on our experiments, visualized correlations
20 were obtained between the Hg signal intensity and the gas flows. The present study,
21 therefore, deciphers this procedure by presenting a digital guide between the Hg signal
22 intensity and the gas flow rates.

23 24 **2. Experimental methods**

2.1 Reagents

Hg (NIST SRM 3133) and Tl (NIST SRM 997) standard solutions were purchased from the National Institute of Standards and Technology (NIST, U.S. Department of Commerce). The UM-Almadén secondary Hg standard solution, produced by University of Michigan, USA, was provided by Professor Dongxing Yuan from Xiamen University, China. Ultra-pure acids (HCl and HNO₃) were used to prepare the standard solutions and digest the samples. SnCl₂ (3%, w/w) was prepared in 10% (v/v) HCl. 18.2 MΩ cm water (ELGA LabWater) was used for the preparation of reagents and solutions.

2.2 Digestion of the standard reference materials

NIST SRM 2711a (Montana II Soil) and four igneous rock standard reference materials (SRMs), including BCR-2 (basalt), BHVO-2 (basalt), GSP-2 (granodiorite) and GSR-2 (andesite) were digested for Hg isotopic composition analysis. Briefly, approximate 0.4 g of each SRM were digested using 4 mL of aqua regia (HCl/HNO₃ = 3, v/v) in a water bath (95 °C) for 2 hours, following the method reported previously.¹⁹⁻²¹ Acid blanks were prepared for each test. The blanks of Hg for acids were lower than <20 pg mL⁻¹. The relative standard deviation of sample duplicates was within 10% of the measured values.

2.3 Instrumental setting

Mercury isotope measurements were conducted on a Neptune Plus MC-ICP-MS housed at the University Research Facility in Chemical and Environmental Analysis (UCEA) in the Hong Kong Polytechnic University. The instrument was equipped with the HGX-200 system and an Aridus II Desolvating Nebulizer System (CETAC Technologies, USA) for Hg and Tl introduction, respectively. SnCl₂ was continually pumped along

1 with Hg(II) solutions and allowed to mix prior to be introduced into the HGX-200
2 system, producing gaseous elemental Hg(0). In the chamber of HGX-200, the Hg(0)
3 was mixed with the dry Tl aerosol generated by the Aridus II desolvating nebulizer
4 before being introduced into the plasma (Fig. 1a). A computer-controlled
5 Perimax Spetec peristaltic pump (Spetec GmbH, Germany) and a PFA-50 nebulizer
6 were used for uptake Hg and Tl solutions, with the uptake rates of about 0.63 mL min⁻¹
7 and 0.05 mL min⁻¹, respectively.

8
9 As shown in Figure 1b-1, the “additional gas 2”, which is used for delivering Tl aerosols
10 from the Aridus II desolvating nebulizer, was originally connected to left side of HGX-
11 200. The “sample gas”, which is for delivering Hg(0) vapor, was originally connected
12 to the right side of HGX-200. We found that such connection generated fluctuate Hg
13 signals. The fluctuated Hg signals may be explained by the fact that the “additional gas
14 2” usually had much higher flow rates than the “sample gas” (Table 1). The higher flow
15 rates of “additional gas 2” caused relatively higher pressure in the chamber, which tends
16 to suppress the pass of “sample gas” through the chamber. In this circumstance, the
17 “sample gas” accumulated and the pressure increased below the chamber. When the
18 accumulated pressure surpassed the pressure in the chamber, the “sample gas” quickly
19 breaks through the chamber. Then the accumulation continued below the chamber until
20 another break through, which caused the fluctuated Hg signal. To solve the problem,
21 the Teflon filter originally located in the middle of chamber was removed (note that
22 many studies did not use filter in their Hg introduction system), and the tubing of
23 “additional gas 2” was extended below the chamber (Fig. 1b-2). After these changes,
24 the “additional gas 2” mixed well with "sample gas" before entering the chamber, and
25 therefore giving stable Hg signals.

2.4 Mercury isotope determination

The NIST SRM 997 Tl standard ($^{205}\text{Tl}/^{203}\text{Tl}=2.38714$) was used as an internal standard for simultaneous instrument mass bias correction of Hg. The nine faraday cups L4, L3, L2, L1, C, H1, H2, H3 and H4 were used to monitor the ^{198}Hg , ^{199}Hg , ^{200}Hg , ^{201}Hg , ^{202}Hg , ^{203}Tl , ^{204}Hg , ^{205}Tl and ^{206}Pb isotopes, respectively. The nickel X skimmer cone combined with the jet cone was employed in the tests. Hg and Tl concentrations in solutions were monitored using ^{202}Hg and ^{205}Tl signal intensities. The signal intensity of ^{202}Hg was approximately 10 mV for 10% (v/v) acid blanks. Isobaric interference of ^{204}Pb to ^{204}Hg was evaluated by measuring the signal intensity of ^{206}Pb , which was $<10^{-4}$ V during the analytical session, suggesting limited interference of ^{204}Pb to ^{204}Hg .

The gains of the amplifier associated with each Faraday collector were calibrated for efficiency on a daily basis. Instrumental parameters (e.g., gas flows, torch settings, and lens system) were tuned to guarantee steady signals, high intensities and good peak shapes. Data were acquired using 2.097 seconds per cycle, similar to previous studies.^{5,18} ASX-112FR Flowing Rinse Micro Autosampler (CETAC Technologies) was employed for every test. Between samples, the autosampler was rinsed using 3% (v/v) HNO_3 for 3.5 minutes until Hg signal intensity returned to the background level. Following the protocol by Blum and Bergquist,⁶ the sample-standard bracketing (SSB) approach was used to compare relative per mil (‰) deviation (using the δ notation) of all our measurements to NIST SRM 3133, according to equation (1):

$$\delta^{\text{xxx}}\text{Hg} (\text{‰}) = [(\text{xxxHg}/^{198}\text{Hg}_{\text{sample}})/(\text{xxxHg}/^{198}\text{Hg}_{\text{NIST3133}})-1] \times 1000 \quad (1)$$

where xxx value is 199, 200, 201, 202 and 204 amu. Hg-MIF is reported in Δ notation ($\Delta^{\text{xxx}}\text{Hg}$, deviation from mass dependency in units of permil, ‰) and is the difference

1 between the measured $\Delta^{xxx}\text{Hg}$ and the theoretically predicted $\Delta^{xxx}\text{Hg}$ value following
2 equations (2-5):

3 $\Delta^{199}\text{Hg} \approx \delta^{199}\text{Hg} - \delta^{202}\text{Hg} \times 0.2520$ (2)

4 $\Delta^{200}\text{Hg} \approx \delta^{200}\text{Hg} - \delta^{202}\text{Hg} \times 0.5024$ (3)

5 $\Delta^{201}\text{Hg} \approx \delta^{201}\text{Hg} - \delta^{202}\text{Hg} \times 0.7520$ (4)

6 $\Delta^{204}\text{Hg} \approx \delta^{204}\text{Hg} - \delta^{202}\text{Hg} \times 1.4930$ (5)

7

8 **3. Results and Discussion**

9

10 *3.1 Effects of “additional gas 2” and “sample gas” flow rates on signal intensities*

11 Four gas flows, i.e., Ar sweep gas and N₂ addition gas of the Aridus II Desolvating
12 Nebulizer System, and “additional gas 2” and “sample gas” of HGX-200 were involved
13 in our method (Fig. 1a). The flow rates of Ar sweep gas and N₂ addition gas were
14 controlled by on-board rotameters, and the flow rates of “additional gas 2” and “sample
15 gas” were controlled by computer. NIST SRM 3133 (1 ng mL⁻¹ Hg in 10% HCl) and
16 NIST SRM 997 (50 ng mL⁻¹ Tl in 3% HNO₃) standard solutions were employed during
17 the test. Based on the initial flow rates of 1.0 L min⁻¹ and 0.3 L min⁻¹ for “additional gas
18 2” and “sample gas”, respectively, the torch position, source lens, zoom optics of MC-
19 ICP-MS, and the Ar sweep gas and N₂ addition gas of the Aridus II Desolvating
20 Nebulizer System, were tuned for a maximum ²⁰²Hg signal intensity. These optimal
21 parameters, as summarized in Table 1, remained unchanged in the later tests.

22

23 To test the effects of “additional gas 2” and “sample gas” flow rates on signal intensities,
24 “additional gas 2” was firstly set to 0 L min⁻¹, and “sample gas” was adjusted to achieve
25 the maximum ²⁰²Hg signal intensity, and the signal intensities of Hg and Tl were

1 recorded. Then the “additional gas 2” was increased to 0.1 L min^{-1} , and the "sample
2 gas" was tuned to reach the maximum ^{202}Hg signal intensity again, and the Hg and Tl
3 signal intensities were also recorded. The above processes were repeated with an
4 incremental of 0.1 L min^{-1} for the “additional gas 2” until it reached to the maximum (2
5 L min^{-1}), which enabled us to build curves (Fig. 2 and 3) to fully understand the effects
6 of “additional gas 2” and "sample gas" flow rates on signal intensities, as shown in
7 Table S1.

8

9 A negatively linear correlation in flow rates was observed between “additional gas 2”
10 and "sample gas" (Fig. 2). Since the “additional gas 2” usually had much higher flow
11 rates than the “sample gas” (Table 1), it indicates that to achieve the highest signal
12 intensity of Hg, high flow rates of “additional gas 2” and low flow rates of “sample gas”
13 were required in the analysis. More interestingly, a positively linear correlation between
14 the flow rate of “additional gas 2” and ^{202}Hg signal intensity (Fig. 3a), and a negatively
15 linear correlation between the flow rate of “sample gas” and ^{202}Hg signal intensity (Fig.
16 3b), were observed. These correlations may be explained by the fact that high flow rates
17 of "sample gas", which delivers $\text{Hg}(0)$ vapor, tend to dilute Hg signals. Although high
18 flow rates of “additional gas 2” also dilute Hg signal, however, the “additional gas 2”
19 carries Tl aerosols. We hypothesize that the Tl aerosols may adsorb a substantial amount
20 of $\text{Hg}(0)$ vapor, which helps to improve the Hg signal intensity. Our hypothesis can be
21 supported by the Hg signal intensity dropped rapidly when the Aridus II Desolvating
22 Nebulizer System introduced air instead of Tl aerosols.

23

24 The change of the flow rates of “additional gas 2” and "sample gas" also affected Tl
25 signal intensities. As shown in Figure 3c, the signal intensity of ^{205}Tl signal was close

1 to zero when the flow rates of “additional gas 2” ranged from 0 to 0.4 L min⁻¹, indicating
2 that limited Tl was delivered with low “additional gas 2” flow rates. As “additional gas
3 2” increased to >0.4 L min⁻¹, ²⁰⁵Tl signals emerged, and their intensities increased until
4 the flow rate of “additional gas 2” reached to 1.0 L min⁻¹ (Fig. 3c). This indicated that
5 the increase of “additional gas 2” flow rate in certain ranges (0.4-1.0 L min⁻¹) was able
6 to increase the delivering of Tl. As the flow rate of “additional gas 2” increased further
7 (1.0-2.0 L min⁻¹), ²⁰⁵Tl signal intensities decreased gradually (Fig. 3c). This indicated
8 that high flow rates of “additional gas 2” (1.0-2.0 L min⁻¹) tended to dilute the Tl signal
9 intensities. The flow rates of "sample gas" showed a mirror image to that of “additional
10 gas 2” (Fig. 3d), which can be explained by the inverse correlation between the two
11 gases (Fig. 2)

12
13 ²⁰²Hg showed consistently linear increase (Fig. 3a) while ²⁰⁵Tl showed a parabolic curve
14 as the “additional gas 2” flow rates increased (Fig. 3c). It can be seen that with the
15 “additional gas 2” flow rate of 1.7 L min⁻¹, ²⁰²Hg and ²⁰⁵Tl had comparable signal
16 intensities. Therefore, 1.7 L min⁻¹ was chosen as the optimized “additional gas 2” flow
17 rate in our method. With this flow rate, the ²⁰²Hg signal sensitivity of 1.78 V per ng mL⁻¹
18 ¹ can be reached when tuning the "sample gas" flow rate to 0.181 L min⁻¹. The high Hg
19 sensitivity (²⁰²Hg: 1.78 V per ng mL⁻¹) at low "sample gas" flow rate may be explained
20 by the removal of the Teflon filter from our introduction system. Mercury has a
21 relatively high ionization potential. Decreasing sample gas flow would permit greater
22 time in plasma for ionization. The remove of the Teflon filter from our introduction
23 system and using the “additional gas 2” created a dilution gas, which could decrease
24 the high gas flow to the plasma, and therefore permitted more efficient ionization of Hg.

3.2 Mercury isotopic determination of low Hg solutions

Based on optimized instrumental conditions (Table 1) and gas flows ("additional gas 2" = 1.7 L min⁻¹; "sample gas" = 0.181 L min⁻¹), UM-Almadén secondary Hg standard solution was diluted to 1.0, 0.7, 0.5, 0.4, 0.3, 0.2, 0.1 ng mL⁻¹ in 10% HCl (v/v) for Hg isotope analysis, using the SSB approach. The bracketed NIST SRM 3133 Hg solutions were diluted to have same Hg concentrations and acid matrices with the UM-Almadén standard. For a certain Hg concentration, replicate measurements (n = 7) were performed. Georg and Newman demonstrated that the use of X skimmer cone with the Neptune Plus MC-ICP-MS may cause the formation of Hg hydrides, which results in an artificial change in ²⁰⁵Tl/²⁰³Tl and mass bias during Hg isotope analysis.⁷ However, a recent study by Yin et al.¹⁸ proved that Hg hydride formation is less important when the Hg isotope measurements are conducted with high Tl concentrations (20-50 ng mL⁻¹ Tl). In our study, NIST SRM 997 (50 ng mL⁻¹ Tl in 3% HNO₃) standard solution was used throughout the analysis.

For both UM-Almadén and NIST SRM 3133 solutions, Hg isotopic ratios (i.e. ¹⁹⁹Hg/¹⁹⁸, ²⁰⁰Hg/¹⁹⁸, ²⁰¹Hg/¹⁹⁸, ²⁰²Hg/¹⁹⁸Hg) increased with the increase of Hg concentrations (Fig. S1), and the uncertainties of Hg isotopic ratios increased with the decrease of Hg concentrations (Fig. 4). Similar patterns have been observed by a previous study.¹⁸ As shown in Table 2 and Fig. 4, when transformed to δ and Δ values, UM-Almadén solutions of 0.3, 0.4, 0.5, 0.7 and 1.0 ng mL⁻¹ showed consistent Hg isotopic composition with previous results,⁶ indicating no anomalous mass bias. However, UM-Almadén solutions of 0.1 ng mL⁻¹ gave more scattered Hg isotopic composition than previous results, and UM-Almadén solutions of 0.2 ng mL⁻¹ showed consistent Hg isotopic composition but with larger standard deviations. It is noteworthy that the above

1 tests were all performed using 3 blocks, 60 cycles per block and 2.097 seconds per cycle.
2 Since each block gave stable and consistent isotopic compositions, we hypothesized
3 that the detection limit can be pushed even lower, by increasing the sample uptake rate,
4 and by decreasing the integration time. Our results showed that the Hg signal intensities
5 can be nearly doubled by increasing the sample uptake rates from 0.63 to 1.26 mL min⁻¹.
6 Only one block (60 cycles, 2.097 seconds per cycle) was used to test the isotopic
7 composition of 0.1 and 0.2 ng mL⁻¹ Hg solutions, with the sample uptake rate of 1.26
8 mL min⁻¹ and 60 seconds of sample introduction time to guarantee stable Hg signal
9 intensities, together with the simultaneous introduction of 50 ng mL⁻¹ Tl. As shown in
10 Table 2, 0.1 and 0.2 ng mL⁻¹ Hg solution then gave comparable results with previous
11 studies.⁶ An additional quality control measure was used for the isotopic analysis of
12 NIST SRM 2711a, which was diluted to 0.1 ng mL⁻¹ Hg. As shown in Table 3, the
13 results obtained during the multiple measurement sessions were in good agreement with
14 previously published results.^{22,23} In this regard, the detection limit of our current system
15 can be confidently set at 0.10 ng mL⁻¹, which, to our knowledge, is the ultimate low
16 value in the available publications.

17
18 The 0.3, 0.4, 0.5, 0.7 and 1.0 ng mL⁻¹ tests were performed using 3 blocks, 60 cycles
19 per block, and 2.097 seconds per cycle, with a total integration time of 380 seconds,
20 plus 90 seconds of sample introduction to guarantee stable Hg signal intensities. The
21 sample uptake was about 0.63 mL min⁻¹, in other words, at least 5.0 mL solution was
22 required to accomplish each test. Similarly, for the 0.1 and 0.2 ng mL⁻¹ tests, it required
23 4.0 mL solution. Since the sample probe of the autosampler cannot reach to the very
24 bottom of the tube, it actually requires 7 mL solution. In fact, the volume of our
25 autosampler tube was 7 mL.

1

2 Considering 7.0 mL of solution was necessary in our method, to obtain a confident Hg
3 isotope data, at least 0.7 ng Hg ($0.10 \text{ ng mL}^{-1} \times 7.0 \text{ mL}$) is required. This was much
4 lower than previous studies that at least 3-20 ng of Hg were used.¹⁸ Considering the
5 acid concentration within each sample should be below 20%, for 7.0 mL diluted
6 solution, the acid should be no more than 1.4 mL, which corresponds to the maximum
7 of 0.14 g of sample used for digestion. In other words, our method can allow the direct
8 measurement of Hg isotopic composition of low Hg samples ($5 \text{ ng g}^{-1} = 0.7 \text{ ng}/0.14 \text{ g}$),
9 using the acid digestion approach. Combined with the available pre-concentration
10 methods,¹⁰⁻¹⁷ the amount of samples and chemicals may be further saved. For example,
11 for very low concentration ($< 5 \text{ ng g}^{-1}$) samples, the analysis needs to pre-concentrate
12 the samples to get 0.70 ng Hg. This is extremely helpful for the measurement of
13 precious samples (e.g., meteorites and aerosol samples) both with low sample size and
14 low Hg concentrations.

15

16 *3.3 Igneous rock reference materials*

17 Igneous rocks are one of the natural materials with low concentration of Hg.²⁴ Four
18 igneous rock SRMs, named BCR-2 (basalt), BHVO-2 (basalt), GSP-2 (granodiorite)
19 and GSR-2 (andesite), were digested and tested for Hg isotopic compositions. The Hg
20 concentration of the SRMs ranged from 6.0 to 22.2 ng g^{-1} , according to the ^{202}Hg signal
21 intensities (Table 4). The Hg concentrations of the SRMs are within the range of
22 previous results.²⁵ The SRMs were analyzed repeatedly over separate analytical
23 sessions on different days, with Hg concentration in the digests of 0.12 to 0.44 ng mL^{-1}
24 (Table 4). For solutions with $\text{Hg} > 0.20 \text{ ng mL}^{-1}$, the isotopic compositions were
25 measured using 3 blocks, 60 cycles per block, and 2.097 seconds per cycle, with the

1 sample uptake rate of 0.63 min⁻¹. For solutions with Hg concentration ≤ 0.20 ng mL⁻¹,
2 the isotopic composition were measured using 1 blocks, 60 cycles per block, and 2.097
3 seconds per cycle, with the sample uptake rate of 1.26 min⁻¹. UM-Almaden was
4 analyzed right after each SRM. The Hg concentrations and acid matrices of NIST SRM
5 3133 were matched to the bracketed samples.

6

7 As shown in Table 4, the long-term reproducibility of the SRMs was comparable to that
8 of the UM-Almadén secondary solutions. The SRMs showed large variations in $\delta^{202}\text{Hg}$
9 (-1.24 to -2.47‰) but little variation in $\Delta^{199}\text{Hg}$ (0.01 to 0.11‰), indicating MDF rather
10 than MIF of Hg isotopes occurred during magmatic processes. Our results about the
11 granodiorite (GSP-2) and andesite (GSR-2) SRMs were similar to that reported for with
12 volcanic rocks of the Clear Lake Volcanic Field, USA ($\delta^{202}\text{Hg}$: -1.20‰ to -0.25‰;
13 $\Delta^{199}\text{Hg}\sim 0$)²⁵, but the basalt SRMs (BCR-2, BHVO-2) showed much lower $\delta^{202}\text{Hg}$
14 values, indicating the isotopic composition in igneous rocks are largely variable, with
15 mafic rocks of lower $\delta^{202}\text{Hg}$, and felsic rocks of higher $\delta^{202}\text{Hg}$.

16

17 **4 Conclusions**

18 Through a modified HGX-200 continuous-flow cold-vapor generation system, and
19 careful optimizations of the instrument gas flows, we obtained steady and high signal
20 sensitivity for Hg, and achieved a detection limit of 0.10 ng mL⁻¹ for the high precision
21 Hg isotope determination. Only 0.70 ng Hg in samples is required using our new
22 method, which enables the direct measurement of low Hg samples (low to 5 ng g⁻¹),
23 after direct acid digestion treatment. Using the developed method, the Hg isotopic
24 compositions of four igneous rock SRMs (BCR-2, BHVO-2, GSP-2, GSR-2) were
25 reported for the first time. The SRMs showed large variations of $\delta^{202}\text{Hg}$, indicating

1 MDF occurred during magmatic processes.

2

3 **Author Contributions**

4 Hongyan Geng and Runsheng Yin contributed equally to this work.

5

6 **Acknowledgements**

7 This work was supported by the University Research Facility in Chemical and
8 Environmental Analysis (UCEA), The Hong Kong Polytechnic University. Runsheng
9 Yin was funded by the Chinese Academy of Sciences through the Hundred Talent Plan.
10 The rock reference materials were generously provided by Prof. Yuan Honglin
11 (Northwest University, Xi'an, China). This work was finically supported by the
12 Research Grants Council (PolyU 152095/14E), and the Natural Science Foundation of
13 China (No. 41602047, 91543205).

References

1. B. A. Bergquist and J.D. Blum, *Elements*, 2009, **5**, 353-357.
2. J. D. Blum, L. S. Sherman and M. W. Johnson, *Annu. Rev. Earth Planet. Sci.*, 2014, **42**, 249-269.
3. R. S. Yin, X. B. Feng, X. D. Li, B. Yu and B. Y. Du, *Trends in Environmental Analytical Chemistry*, 2014, **2**, 1-10.
4. D. S. Lauretta, B. Klaue, J. D. Blum and P. R. Buseck, *Geochim. Cosmochim. Acta*, 2001, **65**, 2807-2818.
5. D. Foucher and H. Hintelmann, *Anal. Bioanal. Chem.*, 2006, **384**, 1470-1478.
6. J. D. Blum and B. Bergquist, *Anal. Bioanal. Chem.*, 2007, **388**, 353-359.
7. R. B. Georg and K. Newman, *J. Anal. At. Spectrom.*, 2015, **30**, 1935-1944.
8. J. Masbou, D. Point and J. E. Sonke, *J. Anal. At. Spectrom.*, 2013, **28**, 1620-1628.
9. J. E. Sonke, T. Zambardi and J. P. Toutain, *J. Anal. At. Spectrom.*, 2008, **23**, 569-573.
10. X. Fu, L. E. Heimbürger and J. E. Sonke, *J. Anal. At. Spectrom.*, 2014, **29**, 841-852.
11. L. E. Gratz, G. J. Keeler, J. D. Blum and L. S. Sherman, *Environ. Sci. Technol.*, 2010, **44**, 7764-7770.
12. L. S. Sherman, J. D. Blum, Joel D. G. J. Keeler, J. D. Demers, J. T. Dvornch, *Environ. Sci. Technol.*, 2012, **46**, 382-390.
13. W. Zheng and H. Hintelmann, *J. phys. chem. A*, 2010, **114**, 4238-4245.
14. J. D. Demers, J. D. Blum and D. R. Zak, *Global Biogeochemical Cycles*, 2013, **27**, 222-238.
15. J. M. Rolison, W. M. Landing, W. Luke, M. Cohen and V. J. M. Salters, *Chem. Geol.*, 2013, **336**, 37-49.
16. H. Y. Lin, D. X. Yuan, B. Y. Lu, S. Y. Huang, L. M. Sun, F. Zhang and Y. Q. Gao, *J. Anal. At. Spectrom.*, 2015, **30**, 353-359.
17. M. Štok, H. Hintelmann and B. Dimock, *Anal. Chim. Acta*, 2014, **851**, 57-63.
18. R. S. Yin, D. P. Krabbenhoft, B. A. Bergquist, W. Zheng, R. F. Lepak and J. P. Hurley, *J. Anal. At. Spectrom.*, 2016, **31**, 2060-2068.
19. J. Chen, H. Hintelmann and B. Dimock, *J. Anal. At. Spectrom.*, 2010, **25**, 1402-1409.
20. R. S. Yin, X. B. Feng and J. B. Chen, *Environ. Sci. Technol.*, 2014, **48**, 5565-5574.
21. J. L. Liu, X. B. Feng, R. S. Yin, W. Zhu and Z. G. Li, *Chem. Geol.*, 2011, **287**, 81-89.
22. L. S. Sherman, J. D. Blum, D. K. Nordstrom, R. B. McCleskey, T. Barkay and C. Vetriani, *Earth Planet. Sci. Lett.*, 2009, **279**, 86-96.
23. J. Gray, M. Pribil, P. Van Metre, D. Borrok and A. Thapalia, *Applied Geochemistry*, 2013, **29**, 1-12.
24. R. Y. Sun, M. Enrico, L. E. Heimbürger, C. Scott and J. Sonke, *Anal. Bioanal. Chem.*, 2013, **405**, 6771-6781.
25. C. N. Smith, S. E. Kesler, J. D. Blum and J. J. Rytuba, *Earth Planet. Sci. Lett.*, 2008, **269**, 399-407.

Table 1 Operating parameters for Hg isotope analysis

MC-ICP-MS	
Cool gas (Ar)	16.00 L min ⁻¹
Auxiliary gas (Ar)	0.8 L min ⁻¹
Sample gas (Ar)	0.181 L min ⁻¹
Additional gas 2 (Ar)	1.7 L min ⁻¹
X-Pos	-3.76 mm
Y-Pos	-1.76 mm
Z-Pos	-3.43 mm
RF power	1200 W
Extraction	-1610 V
Focus	-502 V
X-Defl	6.49 V
Y-Defl	-0.73 V
Shape	208 V
Rot Quad 1	6.07 V
Source Offset	1.00 V
Focus Quad	10 V
Dispersion Quad	0 V
Aridus II	
Nebulizer	PFA-50
Sweep gas (Ar)	3.31 L min ⁻¹
Addition gas (N ₂)	0 L min ⁻¹

Table 2 Hg isotope composition of UM-Almadén. The tests for 0.1 and 0.2 ng mL⁻¹ solutions were performed with the sample uptake rate of 1.26 mL min⁻¹, and using 1 block, 60 cycles per block and 2.097 seconds per cycle. The tests for other solutions were performed with the sample uptake rate of 0.63 mL min⁻¹, and using 3 blocks, 60 cycles per block and 2.097 seconds per cycle.

Hg concentration (ng mL ⁻¹)	$\delta^{199}\text{Hg}$ (‰)	$\delta^{200}\text{Hg}$ (‰)	$\delta^{201}\text{Hg}$ (‰)	$\delta^{202}\text{Hg}$ (‰)	$\Delta^{199}\text{Hg}$ (‰)	$\Delta^{200}\text{Hg}$ (‰)	$\Delta^{201}\text{Hg}$ (‰)
0.1	-0.20	-0.37	-0.42	-0.54	-0.07	-0.10	-0.01
	-0.16	-0.31	-0.42	-0.55	-0.02	-0.03	0.00
	-0.10	-0.19	-0.26	-0.48	0.02	0.05	0.11
	-0.13	-0.22	-0.33	-0.52	0.00	0.04	0.06
	-0.05	-0.23	-0.39	-0.47	0.07	0.00	-0.03
	-0.11	-0.25	-0.35	-0.48	0.01	-0.01	0.01
	-0.11	-0.25	-0.40	-0.53	0.03	0.02	0.00
	-0.11	-0.26	-0.47	-0.61	0.05	0.05	-0.01
Average	-0.12	-0.26	-0.38	-0.52	0.01	0.00	0.01
SD	0.04	0.06	0.07	0.05	0.04	0.05	0.05
0.2	-0.10	-0.24	-0.33	-0.50	0.00	0.00	0.00
	-0.11	-0.25	-0.39	-0.50	0.01	0.00	-0.02
	-0.13	-0.19	-0.33	-0.47	-0.01	0.05	0.03
	-0.14	-0.31	-0.38	-0.49	-0.01	-0.06	-0.01
	-0.12	-0.25	-0.38	-0.51	0.01	0.01	0.00
	-0.16	-0.31	-0.42	-0.55	-0.02	-0.03	0.00
	-0.04	-0.25	-0.34	-0.50	0.08	0.00	0.04
	-0.16	-0.31	-0.42	-0.55	-0.02	-0.03	0.00
Average	-0.12	-0.26	-0.37	-0.51	0.01	-0.01	0.00
SD	0.04	0.04	0.04	0.03	0.03	0.03	0.02
0.3	-0.11	-0.27	-0.49	-0.46	-0.03	-0.02	0.03
	-0.12	-0.30	-0.45	-0.48	0.02	0.01	0.03
	-0.10	-0.24	-0.33	-0.49	0.02	0.01	0.03
	-0.13	-0.24	-0.35	-0.47	-0.01	0.00	0.00
	-0.16	-0.31	-0.42	-0.55	-0.02	-0.03	0.00
	-0.07	-0.23	-0.46	-0.55	0.07	0.05	-0.05
	-0.09	-0.28	-0.39	-0.56	0.05	-0.01	0.03
	-0.17	-0.25	-0.39	-0.48	-0.05	-0.01	-0.03
Average	-0.12	-0.26	-0.41	-0.51	0.01	0.00	0.01
SD	0.03	0.03	0.05	0.04	0.04	0.02	0.03
0.4	-0.10	-0.19	-0.28	-0.48	0.02	0.05	0.08
	-0.14	-0.26	-0.34	-0.48	-0.02	-0.02	0.02
	-0.15	-0.29	-0.35	-0.47	-0.03	-0.05	0.01
	-0.12	-0.23	-0.33	-0.48	0.00	0.01	0.03
	-0.14	-0.30	-0.42	-0.58	0.00	-0.01	0.01
	-0.19	-0.27	-0.43	-0.52	-0.06	0.00	-0.04
	-0.12	-0.24	-0.41	-0.50	0.00	0.02	-0.03
	-0.15	-0.26	-0.45	-0.52	-0.02	0.00	-0.06
Average	-0.14	-0.25	-0.38	-0.50	-0.01	0.00	0.00
SD	0.03	0.03	0.06	0.03	0.03	0.03	0.04
0.5	-0.14	-0.25	-0.40	-0.52	-0.01	0.01	-0.01
	-0.13	-0.25	-0.40	-0.50	-0.01	0.00	-0.02

	-0.14	-0.26	-0.42	-0.55	0.00	0.02	-0.01
	-0.13	-0.29	-0.45	-0.58	0.01	0.00	-0.01
	-0.13	-0.25	-0.41	-0.50	-0.01	0.00	-0.03
	-0.12	-0.26	-0.43	-0.49	0.01	-0.02	-0.06
	-0.15	-0.28	-0.37	-0.47	-0.04	-0.04	-0.02
	-0.13	-0.27	-0.35	-0.49	0.00	-0.02	0.02
Average	-0.13	-0.26	-0.40	-0.51	0.00	-0.01	-0.02
SD	0.01	0.02	0.03	0.04	0.01	0.02	0.02
0.7	-0.12	-0.25	-0.38	-0.51	0.01	0.01	0.00
	-0.11	-0.25	-0.40	-0.53	0.03	0.02	0.00
	-0.15	-0.28	-0.46	-0.55	-0.02	0.00	-0.05
	-0.18	-0.26	-0.44	-0.57	-0.03	0.02	-0.01
	-0.11	-0.25	-0.35	-0.48	0.01	-0.01	0.01
	-0.11	-0.23	-0.43	-0.54	0.03	0.04	-0.03
	-0.12	-0.25	-0.38	-0.51	0.01	0.01	0.00
	-0.11	-0.25	-0.40	-0.53	0.03	0.02	0.00
Average	-0.12	-0.25	-0.41	-0.53	0.01	0.01	-0.01
SD	0.03	0.01	0.03	0.03	0.02	0.01	0.02
1	-0.12	-0.28	-0.43	-0.56	0.02	0.01	-0.01
	-0.11	-0.25	-0.41	-0.56	0.03	0.03	0.01
	-0.12	-0.24	-0.40	-0.53	0.02	0.03	0.00
	-0.11	-0.24	-0.42	-0.54	0.03	0.03	-0.01
	-0.14	-0.28	-0.45	-0.51	-0.01	-0.03	-0.06
	-0.14	-0.24	-0.41	-0.54	0.00	0.03	-0.01
	-0.11	-0.25	-0.39	-0.50	0.02	0.01	-0.01
	-0.08	-0.24	-0.45	-0.51	0.05	0.02	-0.07
Average	-0.11	-0.25	-0.42	-0.53	0.02	0.02	-0.02
SD	0.02	0.02	0.02	0.02	0.02	0.02	0.03

Table 3 Hg isotope composition of 0.1 ng mL⁻¹ SRM NIST 2711a (Montana II soil). The tests were performed with the sample uptake rate of 1.26 mL min⁻¹, and using 1 block, 60 cycles per block and 2.097 seconds per cycle.

	$\delta^{199}\text{Hg}$ (‰)	$\delta^{200}\text{Hg}$ (‰)	$\delta^{201}\text{Hg}$ (‰)	$\delta^{202}\text{Hg}$ (‰)	$\Delta^{199}\text{Hg}$ (‰)	$\Delta^{200}\text{Hg}$ (‰)	$\Delta^{201}\text{Hg}$ (‰)
	-0.22	-0.03	-0.25	-0.09	-0.19	0.01	-0.18
	-0.23	-0.07	-0.26	-0.08	-0.21	-0.03	-0.20
	-0.24	-0.10	-0.26	-0.11	-0.21	-0.04	-0.17
	-0.22	-0.06	-0.26	-0.08	-0.20	-0.02	-0.20
	-0.28	-0.08	-0.26	-0.12	-0.25	-0.02	-0.17
	-0.23	-0.06	-0.26	-0.14	-0.19	0.01	-0.15
	-0.28	-0.08	-0.27	-0.07	-0.26	-0.04	-0.22
	-0.23	-0.04	-0.22	-0.07	-0.21	0.00	-0.17
Average	-0.24	-0.07	-0.25	-0.10	-0.22	-0.02	-0.18
SD	0.02	0.02	0.01	0.03	0.02	0.02	0.02

Table 4 Hg isotope compositions of the igneous rock SRMs

SRM	N	Hg	Hg	$\delta^{199}\text{Hg}$	SD	$\delta^{200}\text{Hg}$	SD	$\delta^{201}\text{Hg}$	SD	$\delta^{202}\text{Hg}$	SD	$\Delta^{199}\text{Hg}$	SD	$\Delta^{200}\text{Hg}$	SD	$\Delta^{201}\text{Hg}$	SD
		(ng g ⁻¹)	(ng mL ⁻¹)	(‰)	(‰)	(‰)	(‰)	(‰)	(‰)	(‰)	(‰)	(‰)	(‰)	(‰)	(‰)	(‰)	(‰)
BCR-2	5	6.8	0.14	-0.52	0.07	-1.04	0.04	-1.56	0.04	-2.08	0.04	0.00	0.07	0.01	0.04	0.00	0.07
BHVO-2	5	6.0	0.12	-0.65	0.05	-1.24	0.06	-1.84	0.04	-2.44	0.05	-0.03	0.04	-0.01	0.06	0.00	0.03
GSP-2	5	22.2	0.44	-0.29	0.08	-0.59	0.12	-0.88	0.11	-1.20	0.11	0.01	0.07	0.02	0.07	0.02	0.06
GSR-2	5	11.5	0.23	-0.26	0.06	-0.69	0.12	-1.09	0.19	-1.47	0.13	0.11	0.03	0.05	0.07	0.02	0.12

Figure Captions

Fig. 1 (a) Sketch of the sample introduction system. Figure (b-1) shows the original setting of the tubing of “additional gas2”, which produces fluctuate Hg signals. Figure (b-2) shows the modified setting, where the tubing is extended below and give stable Hg signals.

Fig. 2 Relationship between the flow rates of "additional gas 2" and "sample gas".

Fig. 3 Gas flows vs ^{202}Hg intensity and ^{205}Tl intensity.

Fig. 4 Hg isotopic composition of UM-Almadén with different Hg concentrations. The tests for 0.1 and 0.2 ng mL⁻¹ solutions were performed with the sample uptake rate of 1.26 mL min⁻¹, and using 1 block, 60 cycles per block and 2.097 seconds per cycle. The tests for other solutions were performed with the sample uptake rate of 0.63 mL min⁻¹, and using 3 blocks, 60 cycles per block and 2.097 seconds per cycle. The red diamond shows the average of the eight analyses for each concentration and the bar represents the error of the replicate analyses.

Figure 1

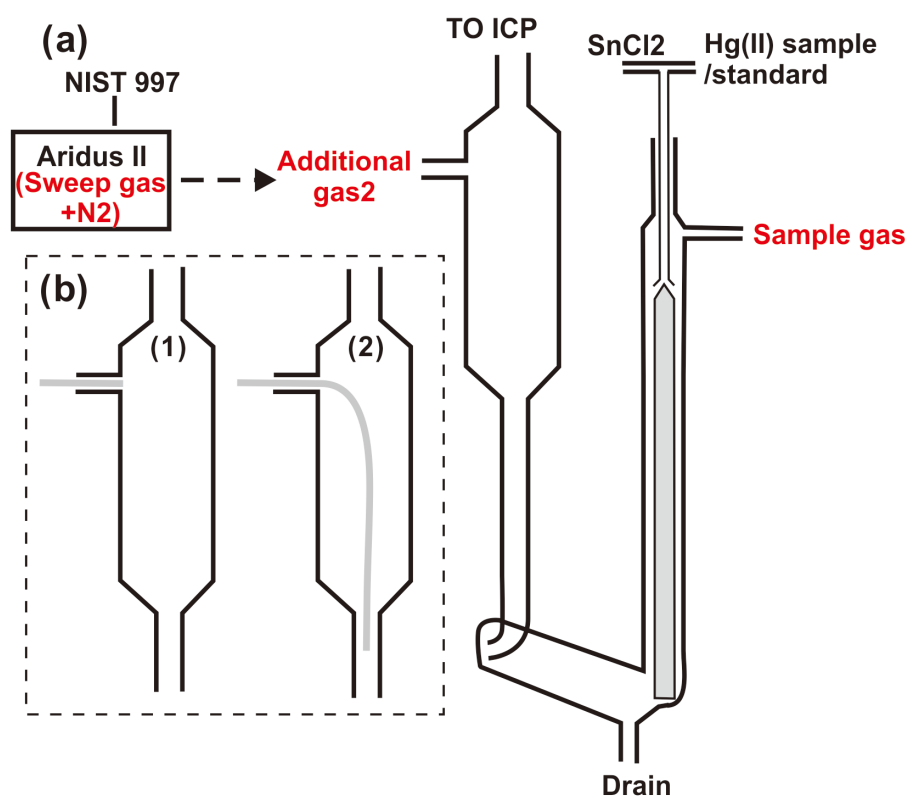


Figure 2

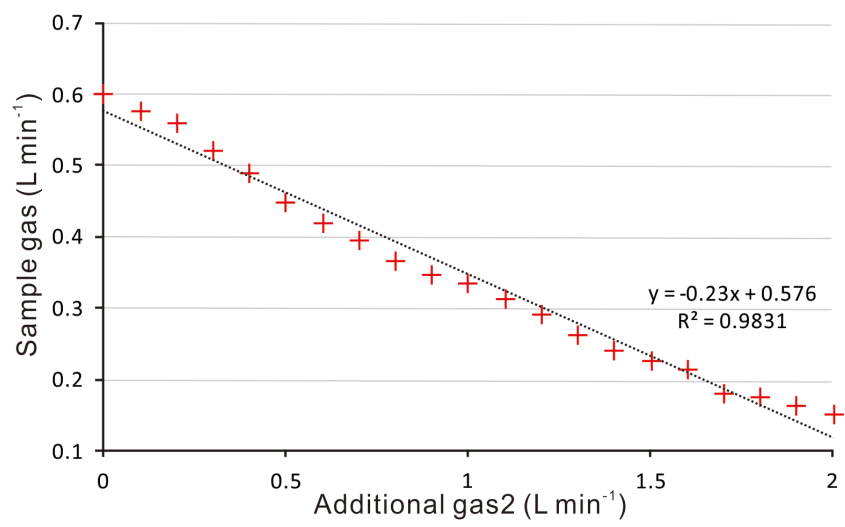


Figure 3

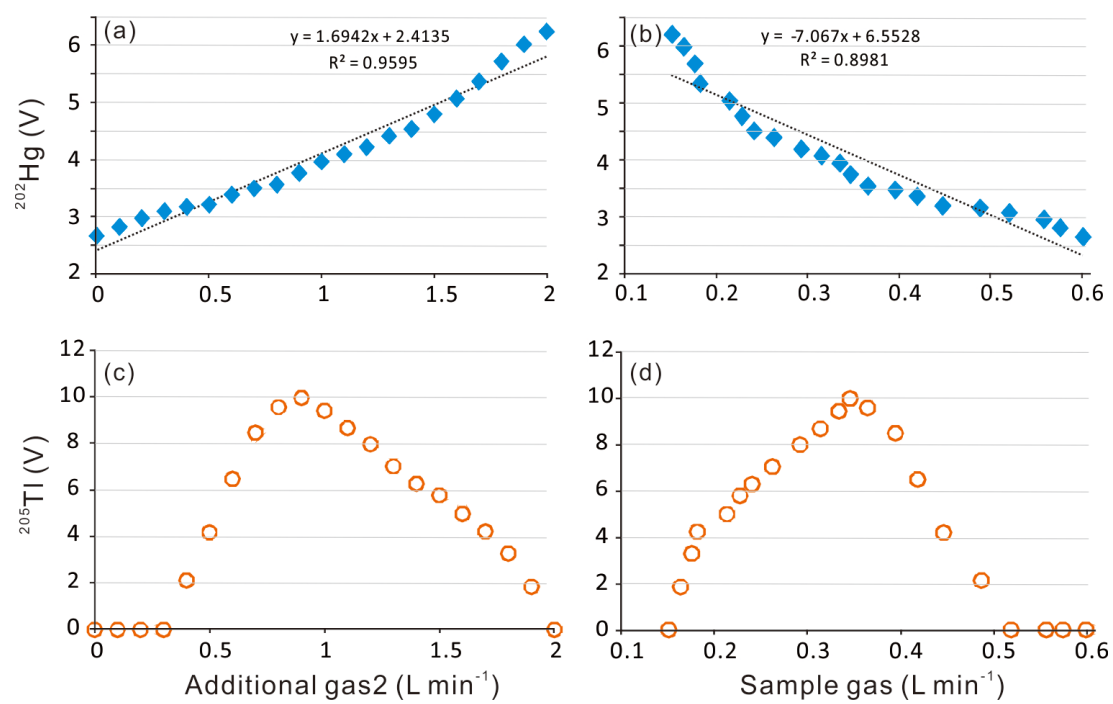


Figure 4

